

## Guided echoes in the magnetosphere: Observations by Radio Plasma Imager on IMAGE

Shing F. Fung,<sup>1</sup> Robert F. Benson,<sup>1</sup> Donald L. Carpenter,<sup>2</sup> James L. Green,<sup>1</sup> Venku Jayanti,<sup>3</sup> Ivan A. Galkin,<sup>4</sup> and Bodo W. Reinisch<sup>4</sup>

Received 28 October 2002; revised 5 March 2003; accepted 10 March 2003; published 12 June 2003.

[1] Long-range, discrete, radio echo traces observed in the magnetosphere by the Radio Plasma Imager (RPI) on IMAGE have been interpreted as signals guided along geomagnetic field lines. During IMAGE traversals of the plasmopause and near-equatorial plasmasphere, multiple echo traces, attributed to signals reflected successively between conjugate hemispheres, are often observed. Single traces seen far beyond the plasmopause at high latitudes are attributed to guided echoes from the local hemisphere in the polar region. Here the field lines are either (1) open, (2) closed but too long to be observed within the instrument listening time or (3) closed but not able to maintain the signal-guiding conditions across the equator to the conjugate hemisphere. In this letter we present examples of guided echoes producing both the single and multiple reflection traces observed by RPI at altitudes of a few Earth radii and discuss possible guiding mechanisms. *INDEX*

*TERMS:* 2730 Magnetospheric Physics: Magnetosphere—inner; 2740 Magnetospheric Physics: Magnetospheric configuration and dynamics; 2768 Magnetospheric Physics: Plasmasphere; 2736 Magnetospheric Physics: Magnetosphere/ionosphere interactions; 2799 Magnetospheric Physics: General or miscellaneous.

**Citation:** Fung, S. F., R. F. Benson, D. L. Carpenter, J. L. Green, V. Jayanti, I. A. Galkin, and B. W. Reinisch, Guided echoes in the magnetosphere: Observations by Radio Plasma Imager on IMAGE, *Geophys. Res. Lett.*, 30(11), 1589, doi:10.1029/2002GL016531, 2003.

### 1. Introduction

[2] The Radio Plasma Imager (RPI) on the IMAGE satellite performs long-range magnetospheric radio sounding [Reinisch *et al.*, 2000]. Before launch, ray-tracing studies produced discrete plasmagram traces of direct high-frequency electromagnetic wave echoes, particularly from over the polar cap and near the plasmopause regions [Green *et al.*, 2000]. After launch, the RPI-observed discrete-echo traces were attributed primarily to field-aligned propagation [Reinisch *et al.*, 2001a, 2001b; Carpenter *et al.*, 2002]. Here we demonstrate the widespread occurrences of these field-aligned echoes throughout the magnetosphere, and discuss

the occurrence-frequency implications in terms of guidance by field-aligned electron density irregularities (FAI).

[3] Calvert [1981] suggested that *R-X* waves ducted in FAI would be readily detectable. Evidence of ducting has been observed in the ionosphere for *L-O* and *R-X* modes [see, e.g., Muldrew, 1963, 1967, 1980] and in the magnetosphere for whistlers [e.g., Angerami, 1970; Carpenter, 1981; Carpenter and Sulic, 1988]. Only a few percent  $N_c$  enhancement is required for effective whistler ducting [e.g., Smith, 1961; Helliwell, 1965], and a similar  $N_c$  depletion for *L-O* and *R-X* mode ducting [see, e.g., Muldrew, 1963, 1967; Platt and Dyson, 1989; Calvert, 1995]. Oya *et al.* [1990] attributed HF wave echoes observed at a radial distance of  $\sim 1.9 R_E$  to ducting. FAI can also cause aspect-sensitive coherent scattering normal to the magnetic field [e.g., Fejer and Kelley, 1980; Fung *et al.*, 2000], yielding *Spread-F* type HF-radar signatures [e.g., James, 1989].

[4] Ducting, however, is not the only proposed mechanism for the RPI discrete traces. In a case study of discrete echoes from conjugate hemispheres, Reinisch *et al.* [2001b] showed that they were due to field-aligned propagation. This propagation would result naturally for waves with small wave normal angles, if the refractive index gradient is nearly field aligned. This situation is possible, for example, within regions where diffusive equilibrium is maintained along  $\mathbf{B}$ , or over the polar cap region where  $N_c$  falls off monotonically essentially along radial field lines. It is unclear, however, how such conditions may occur within the plasmasphere near the equator where substantial cross-field density gradients are known to exist on spatial scales  $\geq 200$  km [e.g., Carpenter and Anderson, 1992]. Here we refer to the discrete echo traces, from either ducting or a field-aligned refractive index gradient, as simply due to guided echoes.

### 2. Guided and Direct Echoes Near Plasmopause

[5] Figure 1a shows guided echo traces observed just outside the plasmopause as determined from RPI passive plasma wave observations [e.g., Fung *et al.*, 2002]. Direct echoes from the plasmopause at 110–200 kHz have a relatively constant virtual range  $\sim 0.8 R_E$ , consistent with the short plasmopause distance ( $0.5 R_E$ ) before entry. The diffuse appearance is attributed to coherent scattering from plasma irregularities in the plasmopause region [Carpenter *et al.*, 2002]. Direct plasmaspheric echoes appear at higher frequencies (300–500 kHz). Their range-spread of  $\sim 0.5 R_E$  (compared to typical  $\sim 960$  km guided echo trace widths, strongly suggests the widespread presence of FAI.

[6] The discrete 80–200 kHz trace in Figure 1a extends to a much greater virtual range than the nearby plasmopause direct echoes at the same frequencies. The asymptotic

<sup>1</sup>NASA Goddard Space Flight Center, Greenbelt, Maryland, USA.

<sup>2</sup>Space, Telecommunications, and Radioscience Laboratory, Stanford University, Stanford, California, USA.

<sup>3</sup>Raytheon Information Technology and Scientific Services/NASA Goddard Space Flight Center, Greenbelt, Maryland, USA.

<sup>4</sup>Center for Atmospheric Research, University of Massachusetts, Lowell, Massachusetts, USA.

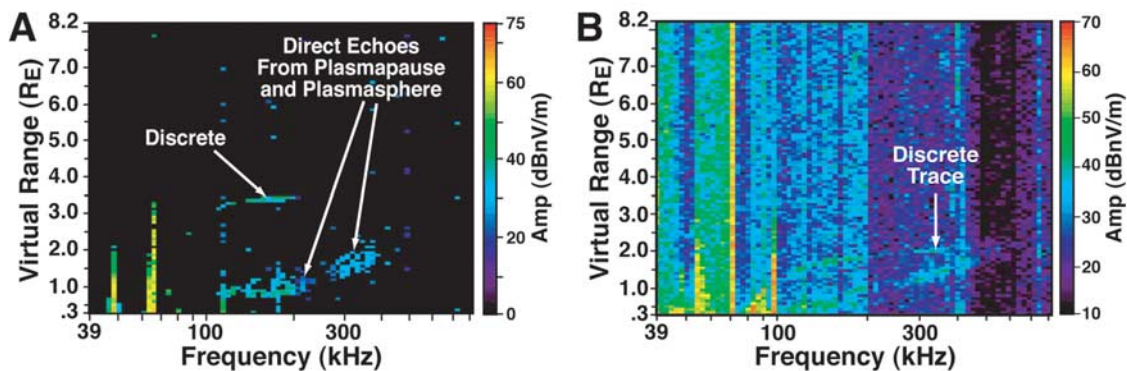


**Figure 1.** Guided and direct echoes from the plasmopause and plasmasphere observed during (a) inbound on Jan 18, 2001, 0239:20 UT ( $L = 5.0$ ,  $R = 4 R_E$ ,  $26^\circ$  MLAT, 16.4 MLT),  $\sim 15$  min prior to plasmopause entry ( $L_P = 4.1$ ), and (b) outbound on Jan 19, 2001, 0935:15 UT ( $L = 6.9$ ,  $R = 3 R_E$ ,  $50^\circ$  MLAT, 5.2 MLT),  $\sim 5$  minutes beyond the plasmopause ( $L_P = 5.6$ ). These plasmagrams cover 40–800 kHz in 78 4%-logarithmic steps in 46 s. A 9 dB “most probable noise” has been subtracted frequency-by-frequency in (a), but not in (b). The “vertical bars” extending to a few  $R_E$  are RPI-stimulated resonances. The resonances in (a) at 48.7, 66.6, 81.0, 115.3, and 177.6 kHz are the 3rd, 4th, 5th, 7th, and 11th gyroharmonics. The average gyro-frequency over the partial frequency scan is 16.34 kHz, while the corresponding model gyro-frequency is 16.21 kHz. The gyroharmonics at 48.7 and 98.6 kHz in (b) correspond to the 1st and 2nd harmonics of the average gyro-frequency at 49.1 kHz, in reasonable agreement with a model value of 49.9 kHz.

approach to a maximum virtual range at high frequencies indicates progressively sharper density and magnetic-field gradients at larger ranges. The only reasonable path for such long-range echoes is one that follows a magnetic flux tube toward lower altitudes in the high-latitude ionosphere [Reinisch *et al.*, 2001b]. The comparable signal strengths ( $>120$  kHz) of the discrete echoes and shorter-range direct echoes indicate little path loss for the discrete signals.

[7] Figure 1b shows guided (discrete) and direct (spread) echoes observed just outside the plasmopause. Nearly the same upper-frequency limit of  $\sim 600$  kHz are present on each (visible in the original data), suggesting nearly the same  $N_e$  level ( $\sim 4 \times 10^3 \text{ cm}^{-3}$ ) at different locations. Although both echoes have nearly the same upper virtual range ( $\sim 2 R_E$ ), the guided echoes must have longer path lengths and are reflected at lower altitudes than the direct signals at the same frequency. The “parabolic” shape of the discrete trace is consistent with having low  $N_e$  along much of the field line at high altitudes, with sharply increasing  $N_e$  toward low

altitudes in the high-latitude ionosphere [Reinisch *et al.*, 2001b]. The nearly linear virtual range-frequency relationship of the direct-echo trace on the other hand suggests a nearly constant  $N_e$  gradient just inside the plasmopause.

[8] Guided echoes observed well outside the plasmopause (Figure 2) with virtual ranges of  $1.2 R_E$  ( $\sim 42$  kHz) to  $\sim 3.1 R_E$  (137.5 kHz) are due to local hemisphere propagation. The nearly constant virtual range at higher frequencies indicates increasingly steeper  $N_e$  gradients deeper in the polar ionosphere. The traces at  $4.9$ – $5.6 R_E$  and  $7.9$ – $8.6 R_E$  appear between 60 and 90 kHz (see arrows) result from guided signals reflected between conjugate hemispheres (see next section).

[9] A single guided echo trace from the local polar-cap ionosphere is usually seen at high altitudes outside the plasmopause. Figure 3 shows an example (30–300 kHz) observed near  $L = 124$ . Here, it would be difficult to distinguish between field-aligned and vertical reflection traces due to the proximity of the two directions. *Fung et al.* [2002] showed examples of such echo traces appearing repeatedly for three hours.

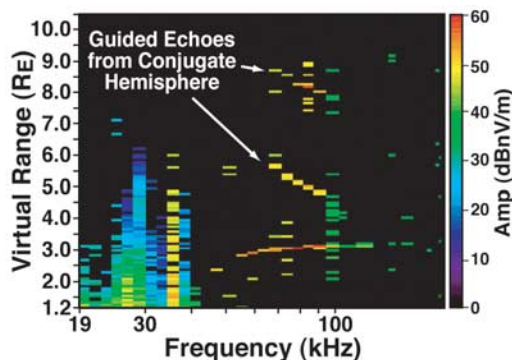


**Figure 2.** Guided echoes from local and conjugate hemispheres seen far outside the plasmopause on March 8, 2001, at 2152:06 UT ( $36.6^\circ$  N,  $13.1$  MLT,  $L = 8.54$ ). The sounding program integrated 4 16-chip pulses per frequency [only 1-chip (3.2 ms) pulse per frequency was used in Figures 1a and 1b].

### 3. Guided Echoes From Conjugate Hemispheres

[10] On closed field lines, guided echoes from conjugate hemispheres can be captured on a plasmagram with suffi-

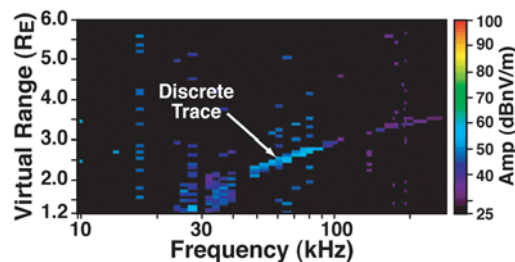


**Figure 3.** Guided echoes observed on June 14, 2000, at 0047:13 UT ( $8.1$  MLT,  $85^\circ$  IL,  $88.9^\circ$  Lat).

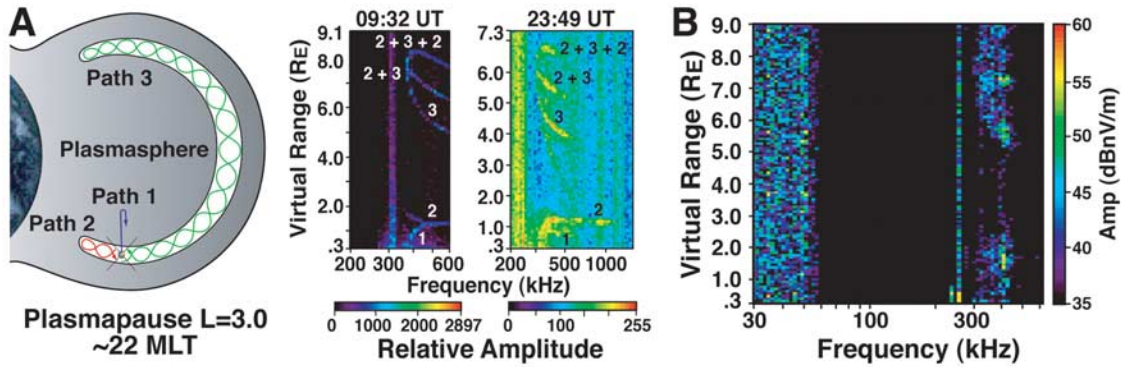


**Figure 4.** “Epsilon” signatures formed by the superposition of successively reflected guided signals from local and conjugate hemispheres. Panel (a) shows exaggerated duct and ray schematics and two epsilons observed on Nov 7, 2000 from nearly the same nighttime location ( $\sim 2 R_E$ ,  $-20^\circ$ – $-25^\circ$  MLAT,  $\sim 22$  MLT,  $L = 2.3$ – $2.6$ ) about one orbital period apart (14.5 hrs). Panel (b) shows a dayside epsilon (10.6 MLT) with spread appearance (Oct 30, 0331:07 UT).

ciently long listening time. Like their ionospheric counterpart [Dyson and Benson, 1978], echoes reflected successively between the local and conjugate hemispheres can form epsilon signatures. Figure 4a shows epsilons observed by two measurement programs (different frequency ranges and gain settings) at nearly identical locations. In each case, trace 1 results from direct echoes from near regions (path 1). Their diffuse appearance suggests aspect-sensitive scattering by plasmaspheric FAI. Traces 2 and 3 are formed by guided signals along paths 2 and 3 in the local and conjugate hemisphere, respectively. An epsilon shape is formed when the local-hemisphere group path (2) is significantly shorter than the conjugate path (3). The mid-section of the epsilon results from guided signals having traveled both paths (2 + 3 and 3 + 2). Trace (2 + 3 + 2) results from an additional round trip along path 2. This interpretation can be verified by adding the virtual ranges of the epsilon components, i.e.,  $(2 + 3) - 2$ ,  $(2 + 3)$  and  $(2 + 3) + 2$ , at each frequency. The two upper traces in Figure 2, pointed out in the previous section, are thus conjugate echoes detected when IMAGE was beyond the plasmopause.

[11] Conjugate end-point conditions will vary with ionospheric conditions and can influence the epsilon appearance. Figure 4b shows a diffuse, but recognizable, epsilon with both the local and conjugate signals appearing coherently scattered or range-spread. Although the epsilons in Figures 4a and 4b were observed in nearly the same magnetic meridian, the nightside ones (22.0 MLT, Figure 4a) appear sharper than the one in the morning sector (10.6 MLT, Figure 4b). The cause of the differences in the dayside and nightside epsilons is not yet known. Additional guided echo examples are shown in Fung et al. [2002].

[12] Conjugate echoes are observed most frequently in the plasmasphere. Figure 5 shows an MLT-distribution of conjugate echo occurrence probability at  $L \leq 4$  determined by the ratio of the plasmagram count having one or more conjugate echo traces to the total plasmagram count recorded. Thus, on average, the conjugate echo occurrence frequency is < a few percent, consistent with ionospheric observations [Muldrew, 1980]. While individual plasmaspheric passes with conjugate echo occurrence probability as high as  $\sim 8$ – $30\%$  have been seen, the low average occurrence probability suggests that the presence of trans-hemispheric guiding may depend on plasmaspheric conditions.

#### 4. Summary and Discussions

[13] Discrete frequency-delay time echo traces observed by RPI have been interpreted as field-aligned guided signals. They are distinguished from direct (spread) echoes by their discreteness when detected near the plasmopause (Figures 1–4). They are widespread in the magnetosphere. While discrete guided echoes can occur inside, near, and outside the plasmopause, epsilon signatures (Figure 4) tend to occur mainly inside the plasmasphere. Conjugate echoes are rarely seen far outside the plasmopause (Figure 2) as the trough tends to be “smoother” by comparison [Carpenter et al., 2002]. The relatively low average conjugate echo occurrence frequency (<3%, Figure 5) may be indicative of the difficulty in maintaining the wave-guiding conditions over most of the field-line length between conjugate hemispheres. Guiding condition maintenance on partial field-line lengths in the local polar ionosphere (Figures 1 and 3) may be easier and thus such cases are more often observed.

[14] As noted above, there are two possible guiding mechanisms: ducting and a field-aligned refractive index gradient. It seems that the efficient guiding seen over the polar region (e.g., Figure 3 and in Fung et al. [2002]) may indeed be due to weak cross-field refractive index variations on field lines having little curvature. Near the magnetic

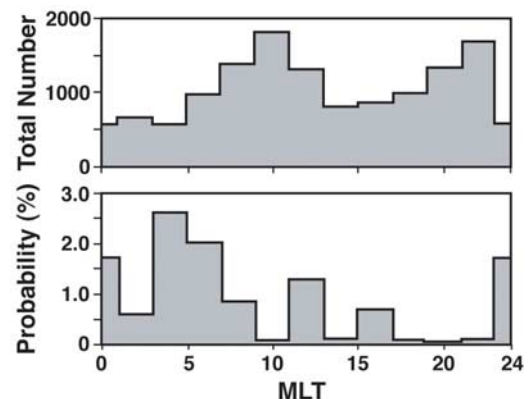


**Figure 5.** Total number of plasmagrams observed at  $L < 4$  during the first 6 months in 2001 (top) and the average occurrence probability of conjugate guided echoes (bottom).

equator, where the field curvature maximizes and the density gradient is directed *across* the field, ducting is the more likely cause of conjugate echoes (Figures 2 and 4).

[15] Observations of scattered echoes, typically attributed to aspect-sensitive scattering by FAI (Figures 1 and 4), also argue against the preponderance of field-aligned refractive index gradients in the magnetosphere and their having a major role in echo guidance. Guided and scattered echoes near the plasmopause and in the plasmasphere reveal different effects of FAI on propagation along and perpendicular to the magnetic field, respectively. *Reinisch et al.* [2001b] demonstrated that guided echoes are due to field-aligned propagation. Here we show that they are observed throughout the magnetosphere. This widespread occurrence of FAI is a picture that has not been well appreciated.

[16] Ducted signals suffer smaller losses than non-ducted signals. Indeed in Figure 1 the discrete echo trace appears stronger than or comparable to the diffuse direct echoes having shorter virtual ranges. Guided signals can propagate from hemisphere to hemisphere (Figures 2 and 4). Figure 2 also shows that the local hemisphere trace extends to both higher (>90 kHz) and lower (<65 kHz) frequencies than the conjugate traces. Thus ducting at the higher and lower frequencies was likely prevented by finite duct variations between conjugate hemispheres.

[17] Figure 4 shows the opposite case where conjugate signals appear weaker than the local-hemisphere signals, suggesting wave energy dissipation over the long conjugate path [*Fung et al.*, 2000]. Figure 4b also indicates the presence of conjugate end point irregularities resulting in the fuzzy epsilon.

[18] Figure 5 in *Fung et al.* [2002] and Figure 4 above clearly reveal guided echoes having signatures very similar to their ionospheric counterparts. It is not clear what processes can produce echo-guiding conditions in the diverse environments of the magnetosphere and ionosphere. The field-aligned propagation properties of the guided echoes make them ideal probes for determining the plasma distributions along geomagnetic field lines, allowing the investigations of field-aligned plasma transport and plasmaspheric refilling processes.

[19] Finally, outer plasmaspheric cross-field irregularity scale sizes can be estimated from the Figure 1. Assuming aspect-sensitive scattering by FAI with cross-field scale sizes  $\leq \lambda/2$ , the plasmopause (100–200 kHz) and outer plasmasphere (300–600 kHz) scattered echoes imply a range of cross-field scales in that combined region of  $\sim 0.25$ –2 km, consistent with *Carpenter et al.* [2002].

## References

Angerami, J. J., Whistler duct properties deduced from VLF observations made with the Ogo 3 satellite near the magnetic equator, *J. Geophys. Res.*, **75**, 6115–6135, 1970.

- Calvert, W., The detectability of ducted echoes in the magnetosphere, *J. Geophys. Res.*, **86**, 1609–1612, 1981.
- Calvert, W., Wave ducting in different wave modes, *J. Geophys. Res.*, **100**, 17,491–17,497, 1995.
- Carpenter, D. L., A study of the outer limits of ducted whistler propagation in the magnetosphere, *J. Geophys. Res.*, **86**, 839–845, 1981.
- Carpenter, D. L., and R. R. Anderson, An ISEE/whistler model of equatorial electron density in the magnetosphere, *J. Geophys. Res.*, **97**, 1097–1108, 1992.
- Carpenter, D. L., and D. M. Sulic, Ducted whistler propagation outside the plasmopause, *J. Geophys. Res.*, **93**, 9731–9742, 1988.
- Carpenter, D. L., M. A. Spasojevic, T. F. Bell, U. S. Inan, B. W. Reinisch, I. A. Galkin, R. F. Benson, J. L. Green, S. F. Fung, and S. A. Boardsen, Small-scale field-aligned plasmaspheric density structures inferred from the Radio Plasma Imager on IMAGE, *J. Geophys. Res.*, **107**(A9), 1258, doi:10.1029/2001JA009199, 2002.
- Dyson, P. L., and R. F. Benson, Topside sounder observations of equatorial bubbles, *Geophys. Res. Lett.*, **5**, 795–798, 1978.
- Fejer, B. G., and M. C. Kelley, Ionospheric irregularities, *Rev. Geophys.*, **18**, 401–454, 1980.
- Fung, S. F., et al., Investigations of irregularities in remote plasma regions by radio sounding: Applications of the Radio Plasma Imager on IMAGE, *Space Sci. Rev.*, **91**, 391–419, 2000.
- Fung, S. F., et al., Observations of magnetospheric plasmas by the Radio Plasma Imager (RPI) on the IMAGE mission, *Adv. Space Res.*, **30**, 2259–2266, 2002.
- Green, J. L., et al., Radio Plasma Imager simulations and measurements, *Space Sci. Rev.*, **91**, 361–389, 2000.
- Helliwell, R. A., *Whistlers and Related Ionospheric Phenomena*, Stanford Univ. Press, Stanford, Calif., 1965.
- James, H. G., ISIS-1 measurements of high-frequency backscatter inside the ionosphere, *J. Geophys. Res.*, **94**, 2617–2629, 1989.
- Muldrew, D. B., Radio propagation along magnetic field-aligned sheets of ionization observed by the Alouette topside sounder, *J. Geophys. Res.*, **68**, 5355–5370, 1963.
- Muldrew, D. B., Medium frequency conjugate echoes observed on topside-sounder data, *Can. J. Phys.*, **45**, 3935–3944, 1967.
- Muldrew, D. B., The formation of ducts and spread F and the initiation of bubbles by field-aligned currents, *J. Geophys. Res.*, **85**, 613–625, 1980.
- Oya, H., et al., Plasma wave observations and sounder experiment (PWS) using the Akebono (EXOS-D) satellite—Instrumentation and initial results, including discovery of the high altitude equatorial plasma turbulence, *J. Geomagn. Geoelectr.*, **42**, 411–442, 1990.
- Platt, I. G., and P. L. Dyson, MF and HF propagation characteristics of ionospheric ducts, *J. Atmos. Terr. Phys.*, **51**, 759–774, 1989.
- Reinisch, B. W., et al., The Radio Plasma Imager investigation on the IMAGE spacecraft, in *The IMAGE Mission*, edited by J. L. Burch, *Space Sci. Rev.*, **91**, (319–359), 2000.
- Reinisch, B. W., et al., First results from the Radio Plasma Imager on IMAGE, *Geophys. Res. Lett.*, **28**, 1167–1170, 2001a.
- Reinisch, B. W., X. Huang, P. Song, G. S. Sales, S. F. Fung, J. L. Green, D. L. Gallagher, and V. M. Vasyliunas, Plasma density distribution along the magnetospheric field: RPI observations from IMAGE, *Geophys. Res. Lett.*, **28**, 4521–4524, 2001b.
- Smith, R. L., Propagation characteristics of whistlers trapped in field-aligned columns of enhanced ionization, *J. Geophys. Res.*, **66**, 3699–3707, 1961.

R. F. Benson, S. F. Fung, and J. L. Green, NASA Goddard Space Flight Center, Greenbelt, MD 20771, USA. (shing.fung@gssc.nasa.gov)

D. L. Carpenter, Space, Telecommunications, and Radioscience Laboratory, Stanford University, Stanford, CA 94305, USA.

I. A. Galkin and B. W. Reinisch, Center for Atmospheric Research, University of Massachusetts, Lowell, MA 01854, USA.

V. Jayanti, Raytheon Information Technology and Scientific Services/NASA Goddard Space Flight Center, Greenbelt, MD 20771, USA.